Inhibition of p-Aminobenzoate and Folate Syntheses in Plants and Apicomplexan Parasites by Natural Product Rubreserine.

Djeneb Camara, Cordelia Bisanz, Caroline Barette, Jeroen van Daele, Esmare Human, Bernice Barnard, Dominique van Der Straeten, Christophe P Stove, Willy E Lambert, Roland Douce, et al.

THE JOURNAL OF BIOLOGICAL CHEMISTRY VOL. 287, NO. 26, pp. 22367–22376, June 22, 2012

Inhibition of *p*-Aminobenzoate and Folate Syntheses in Plants and Apicomplexan Parasites by Natural Product Rubreserine*[S]

Received for publication, March 26, 2012, and in revised form, May 9, 2012 Published, JBC Papers in Press, May 10, 2012, DOI 10.1074/jbc.M112.365833

Djeneb Camara[‡1], Cordelia Bisanz[§], Caroline Barette[¶], Jeroen Van Daele[‖], Esmare Human[**], Bernice Barnard[**], Dominique Van Der Straeten[‡‡2], Christophe P. Stove[‖], Willy E. Lambert[‖2], Roland Douce[‡], Eric Maréchal[‡3], Lyn-Marie Birkholtz[**], Marie-France Cesbron-Delauw[§], Renaud Dumas[‡], and Fabrice Rébeillé[‡4]

From the [‡]Laboratoire de Physiologie Cellulaire Végétale, Commissariat à l'Energie Atomique/CNRS UMR5168/INRA USC1200/Université Joseph Fourier Grenoble I, Institut de Recherches en Technologies et Sciences pour le Vivant, Commissariat à l'Energie Atomique-Grenoble, F-38054 Grenoble, France, the [§]Laboratoire Adaptation et Pathogénie des Microorganismes, CNRS UMR 5163/Université Joseph Fourier Grenoble I, Institut Jean Roget, F-38042 Grenoble, France, the [¶]Centre de Criblage pour Molécules Bioactives, Institut de Recherches en Technologies et Sciences pour le Vivant, Commissariat à l'Energie Atomique-Grenoble, F-38054 Grenoble, France, the [‖]Laboratory of Toxicology, Ghent University, Harelbekestraat 72, B-9000 Ghent, Belgium, the [**]Malaria Research Group, Department of Biochemistry, University of Pretoria, Private Bag x20, Pretoria 0028, South Africa, and the [‡‡]Laboratory of Functional Plant Biology, Department of Physiology, Ghent University, K. L. Ledeganckstraat 35, B-9000 Ghent, Belgium

Background: pABA biosynthesis is a potential target for antifolate drugs.
Results: Rubreserine inhibits GAT-ADCS, an enzyme involved in pABA biosynthesis, and decreases the folate content in *Arabidopsis* and *Toxoplasma.*
Conclusion: Specific inhibition of pABA synthesis induces growth limitation of plants and apicomplexan parasites.
Significance: GAT-ADCS is a valuable target in eukaryotes, and rubreserine is a novel scaffold for anti-parasitic drugs.

Glutamine amidotransferase/aminodeoxychorismate synthase (GAT-ADCS) is a bifunctional enzyme involved in the synthesis of *p*-aminobenzoate, a central component part of folate cofactors. GAT-ADCS is found in eukaryotic organisms autonomous for folate biosynthesis, such as plants or parasites of the phylum Apicomplexa. Based on an automated screening to search for new inhibitors of folate biosynthesis, we found that rubreserine was able to inhibit the glutamine amidotransferase activity of the plant GAT-ADCS with an apparent IC_{50} of about 8 μM. The growth rates of *Arabidopsis thaliana*, *Toxoplasma gondii*, and *Plasmodium falciparum* were inhibited by rubreserine with respective IC_{50} values of 65, 20, and 1 μM. The correlation between folate biosynthesis and growth inhibition was studied with *Arabidopsis* and *Toxoplasma.* In both organisms, the folate content was decreased by 40–50% in the presence of rubreserine. In both organisms, the addition of *p*-aminobenzoate or 5-formyltetrahydrofolate in the external medium restored the growth for inhibitor concentrations up to the IC_{50} value, indicating that, within this range of concentrations, rubreserine was specific for folate biosynthesis. Rubreserine appeared to be more efficient than sulfonamides, antifolate drugs known to inhibit the invasion and proliferation of *T. gondii* in human fibroblasts. Altogether, these results validate the use of the bifunctional GAT-ADCS as an efficient drug target in eukaryotic cells and indicate that the chemical structure of rubreserine presents interesting anti-parasitic (toxoplasmosis, malaria) potential.

Folates are a family of cofactors that are essential for cellular one-carbon (C1) transfer reactions. They are involved in several important metabolic pathways, such as the synthesis of nucleotides and the methylation cycle (1–3). Folate biosynthesis can be divided into three branches (Fig. 1*A*) as follows: the first one is for the pterin ring synthesis; the second one is for the pABA[5] synthesis, and the third one is for the assembly of these two precursors plus glutamates to form the backbone of folate derivatives (4–6). Blocking folate biosynthesis or turnover leads to the arrest of cell division and eventually to cell death. Antifolate drugs have been developed to exploit this feature in therapies against cancer cells and microbial or parasitic infections. Biosynthesis of folate is mainly inhibited by two groups of compounds, *i.e.* inhibitors of dihydropteroate synthase (DHPS) and inhibitors of dihydrofolate reductase (DHFR). Inhibitors of DHFR are commonly used as therapeutic agents against cancer (7), whereas a combination of these two types of inhibitors are

* This work was supported in part the Région Rhône-Alpes (Cluster 9, "Plantacter").
[S] This article contains supplemental Fig. 1.
[1] Ph.D. fellowship was supported by the Région Rhône-Alpes (Cluster 9, "Plantacter").
[2] Supported by Ghent University Grant BOF09-GOA-004.
[3] Supported by an Agence Nationale de la Recherche PlasmoExpress grant.
[4] To whom correspondence should be addressed: PCV/iRTSV, CEA-Grenoble, 17 Ave. des Martyrs, F-38054 Grenoble, France. Tel.: 33-4-38-78-44-93; Fax: 33-4-38-78-50-91; E-mail: frebeille@cea.fr.

[5] The abbreviations used are: pABA, *para*-aminobenzoic acid; GAT-ADCS, glutamine amidotransferase-aminodeoxychorismate synthase; ADCL, aminodeoxychorismate lyase; AS, anthranilate synthase; GMPS, GMP synthetase; GDH, glutamate dehydrogenase; THF, tetrahydrofolate; 5-FTHF, 5-formyl tetrahydrofolate; GAT, glutamine amidotransferase; HFF, human foreskin fibroblast; DHFR, dihydrofolate reductase; DHPS, dihydropteroate synthase; ADC, 4-amino-4-deoxychorismate.

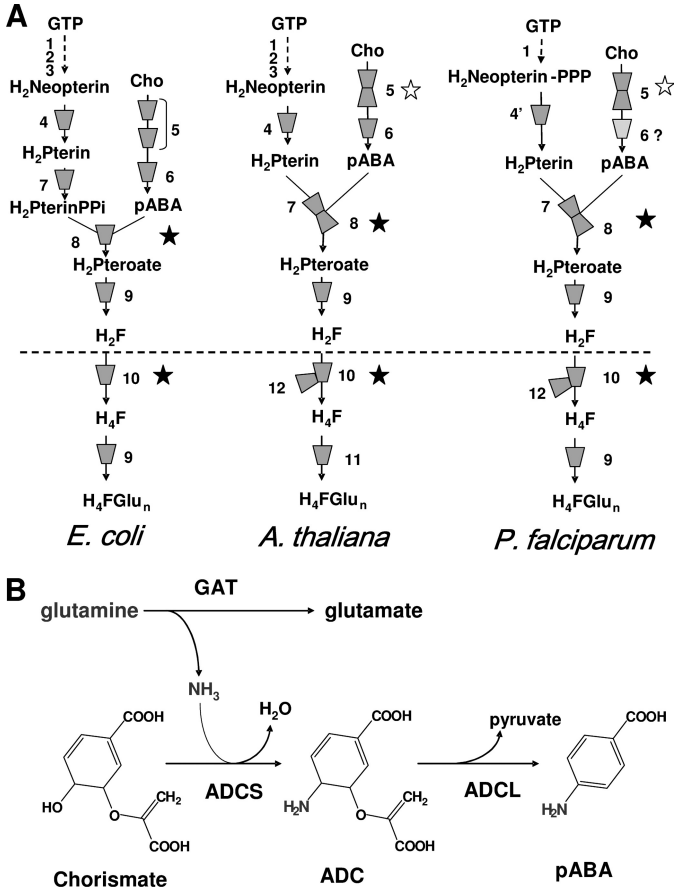

FIGURE 1. **Biosynthesis of THF.** *A,* schematic representation of the pathways found in *E. coli*, *P. falciparum,* and *A. thaliana*. The enzymes involved are as follows: *1,* GTP cyclohydrolase I; *2,* NUDIX hydrolase; *3,* unspecific phosphatase; *4,* dihydroneopterin aldolase; 4′,6-pyruvoyltetrahydropterin synthase; *5,* GAT-ADCS (PabA and PabB in *E. coli*); *6,* ADCL; *7,* 6-hydroxymethyldihydropterin (*H_2Pterin*) pyrophosphokinase; *8,* dihydropteroate (*H_2Pteroate*) synthase; *9,* dihydrofolate (*H_2F*) synthetase; *10,* dihydrofolate reductase; *11,* folylpolyglutamate synthetase; *12,* thymidylate synthase. Other abbreviations: *Cho*, chorismate; *pABA*, *p*-aminobenzoate; *H_2PterinPP*, 6-hydroxymethyldihydropterin pyrophosphate; *H_4F*, tetrahydrofolate; *H_4F-Glu$_n$*, the polyglutamylated form of H_4F. *Merged symbols* represent bifunctional enzymes. The activities *9* and *11* are catalyzed by a single enzyme in *E. coli* and *Plasmodium*. In *Plasmodium*, the activity *6* remains to be identified. Above the *broken line*, the activities are absent in animals. The *black stars* show the two enzymes actually targeted by antifolate drugs. The *white stars* show the potential target studied in this work. *B,* details of the two-step pathway required for pABA synthesis. In all eukaryotes, the first step involves a bifunctional GAT-ADCS, whereas two separate proteins PabA and PabB are found in most (but not all) prokaryotes (19).

commonly used in clinical treatments against parasites of the Apicomplexa phylum, such as *Plasmodium falciparum* or *Toxoplasma gondii* (8, 9). However, the use of these drugs is compromised by the emergence of resistance, and the currently used chemical scaffolds and protein targets are actually overexploited. Nevertheless, the long established efficacy of folate metabolism as a clinical target is strongly encouraging to identify new inhibitors acting against other enzymes of the folate pathway comprising nine enzyme activities in addition to DHPS and DHFR (Fig. 1*A*) (10–12).

Among potential targets, the enzymes involved in the pABA branch of the pathway are of great interest (13). Indeed, they are absent in animals, and the only known metabolic fate of pABA is its commitment in folate synthesis. In addition, it was recently shown in plants that the production of pABA, together with the production of pterins, is rate-limiting for the whole folate pathway (4, 5). Also, it was shown in *P. falciparum* that pABA was an effective salvage substrate in experiments using antifolates, suggesting that pABA metabolism might offer opportunities for chemotherapy (14). The pABA moiety is synthesized in two steps from chorismate (a metabolite also involved in aromatic amino acid synthesis (15)). First, chorismate is aminated to form 4-amino-4-deoxychorismate (ADC), and ADC is then aromatized with loss of pyruvate (Fig. 1*B*). In many bacteria such as *Escherichia coli* or *Bacillus subtilis*, ADC synthesis requires two separate proteins, PabA (a glutamine amidotransferase) and PabB (the ADC synthase) (16). In eukaryotes, the situation appears different. Indeed, in plants and lower eukaryotes, such as yeast and Apicomplexa, ADC synthesis is catalyzed by a single bifunctional protein (Fig. 1*A*) containing two domains, the glutamine amidotransferase (GAT) in the N-terminal part and the ADC synthase (ADCS) in the C terminus (17). Based on sequence similarities with TrpG (the component II of anthranilate synthase), GAT-ADCS is classified as a member of the G-type group of amidotransferases (18, 19). There is only one gene coding for GAT-ADCS in apicomplexan parasites and plants, and a mutation in the plant gene is embryo-defective. The ADCS domain belongs to the group of chorismate-utilizing enzymes, which also contains salicylate synthase, isochorismate synthase, and anthranilate synthase (20, 21). Until now, searches of inhibitors for this class of enzymes were only achieved using prokaryotic systems. They involved docking studies and design of chorismate analogous compounds (22–25), combinatorial chemistry approaches (26, 27), and a specific screening of a microorganism extract collection using growth inhibition of test bacteria as a marker of activity (28, 29). Several compounds were identified by these different methods but appeared to be relatively weak inhibitors of ADCS, although some of them could be quite potent against other chorismate-utilizing enzymes (22–24, 26). The most potent inhibitor of ADCS reported to date is an analog of chorismate (2-hydroxy-4-amino-4-deoxychorismate), exhibiting a K_i value of 38 μM against the purified enzyme (23). To our knowledge, the *in vivo* effects of these ADCS inhibitors have not been investigated.

In this report, using a purified recombinant plant GAT-ADCS as a model enzyme for bifunctional GAT-ADCS, we screened a chemical library for new inhibitors of pABA synthesis. We identified one compound exhibiting a $K_i < 10$ μM and measured the impact of this molecule on a plant (*Arabidopsis thaliana*) and two apicomplexan parasites (*T. gondii* and *P. falciparum*).

EXPERIMENTAL PROCEDURES

Materials—A. thaliana (ecotype Columbia) seedlings were grown on plates containing Murashige and Skoog medium, 15% agar, plus the various molecules to be tested. Seeds were first sterilized by soaking for 15 min in a solution containing 0.095% Tween and 0.57% sodium hypochlorite before placing on the agar medium. The plates were conserved in the dark at 4 °C for 48 h and then transferred in a greenhouse (20 °C, 80% humidity, 150 μmoles photon $m^{-2}\cdot s^{-1}$, 12 h light period). The number of

seedlings at the two leaf stage (rosette stage) was counted after 2 weeks.

A. thaliana (ecotype Columbia) cell suspension cultures were grown and subcultured as described previously (30). For measurements of metabolites, cells were collected after 7 days of treatment, rapidly washed with distilled water, weighted, frozen in liquid nitrogen, and stored at −80 °C for later analyses.

T. gondii tachyzoites from the RH-YFP$_2$ strain (kindly provided by B. Striepen, Athens, GA) were propagated in human foreskin fibroblasts (HFF) under standard procedures as described previously (31). Invasion and proliferation assays were performed on HFF cells grown to confluence on glass coverslips in 4- or 24-multiwell plates. For the invasion assay, freshly egressed RH-YFP$_2$ parasites were incubated for 5 h with or without the different drugs. To perform synchronized invasion, 10^6 parasites/well were centrifuged for 30 s at 1300 rpm onto HFF monolayers, and wells were incubated for 15 min in a water bath at 37 °C. Wells were further washed three times with cold PBS to eliminate extracellular parasites. Infected cells were fixed in 5% formaldehyde/PBS for 30 min and stored in PBS at 4 °C until staining. To distinguish intracellular from remaining extracellular parasites, coverslips were incubated with the primary antibody mAb Tg05-54 against the major *Toxoplasma* surface protein SAG1 (TgSAG1) and then with Texas Red-conjugated goat anti-mouse secondary antibody (Molecular Probes). Intracellular parasites exhibiting a faint red color can easily be distinguished from extracellular parasites that are bright red. Nuclei were stained with Hoechst 33258 (Molecular Probes). The number of intracellular parasites was determined from 12 randomly selected fields per coverslip and per experiment with a Zeiss Axioplan 2 microscope equipped for epifluorescence and phase contrast. Invasion was expressed as percent of the number of intracellular parasites recorded in nontreated cells.

To assess the effect of the drugs on intracellular growth of *T. gondii* (proliferation assay), HFF monolayers were infected with 10^5 parasites/well (*cf.* invasion assay). Wells were then washed three times with PBS to eliminate extracellular parasites, and drugs were added. After 24 h at 37 °C in a humidified atmosphere containing 5% CO_2, cells were fixed and stained with Hoechst 33258 as described above. For each drug concentration, the number of parasites was determined from at least 100 individual vacuoles.

To determine folate concentrations, parasites were grown for 24 h in HFF cells in the presence or absence of 20 or 40 μM rubreserine. The infected HFF monolayers were washed three times with PBS, harvested with a cell scraper, and passed four times through a 27-gauge needle to break the cells. Broken cells and released parasites were washed three times with PBS, and then parasites were purified by filtration through a 3 μm Nucleopore membrane, further washed two times in PBS, concentrated by centrifugation, and frozen at −80 °C until use.

Plasmodium falciparum (3D7) was maintained in human O^+ erythrocytes as described previously (32). The *in vitro* anti-plasmodial activity of the rubreserine was determined using the malaria SYBR Green I fluorescence assay as described previously (33, 34). *In vitro* ring-stage intra-erythrocytic *P. falciparum* parasites (1% hematocrit and 1% parasitemia) were incubated with specific concentrations of rubreserine in complete *P. falciparum* culture medium, with chloroquine disulfate used as a positive control (0.5 μM) or vehicle (1× PBS) as a negative control. Fluorescence was measured after 96 h under drug pressure (excitation 485 nm and emission 538 nm). The data, after subtraction of background (chloroquine disulfate-treated infected RBCs and no parasite growth), were expressed as percentage of untreated control to determine cell proliferation.

Rubreserine Preparation—Rubreserine was prepared from (−)-eseroline fumarate salt (Sigma). Stock solutions of eseroline (10 mM) were made in 50 mM P_i (pH 8), 50 mM Tris (pH 8), or 1× PBS (pH 7.5) buffers, depending on the experiment. Under these conditions, eseroline is spontaneously oxidized into rubreserine, a process completed in about 6 h at room temperature. The formation of rubreserine was controlled through the appearance of a characteristic peak of absorption at 475 nm. These stock solutions were stored at 4 °C for 48 h or at −20 °C for 1 week. They were serially diluted before use.

Expression and Purification of Recombinant Arabidopsis Enzymes—*At*GAT-ADCS and *Ec*ADCL proteins were expressed and purified as described previously (19). *Arabidopsis* cDNAs encoding GMPS, β-subunit of AS starting at Ala-51 to remove the plastid transit peptide, and α-subunit of AS starting at Ala-61 were amplified by PCR and cloned into the expression vector pET28 (Novagen). *E. coli* BL21-CodonPlus (DE3)-RIL cells (Stratagene) were transformed and grown using the same protocol as for *At*GAT-ADCS. Cells were disrupted, and His-tagged recombinant proteins were purified as described previously (19).

Determination of Enzyme Activities—GAT activity can be determined by measuring the production of glutamate and ADCS activity by the production of pABA (19). Standard assays contained 100 mM Tris/HCl (pH 8.0), 5 mM $MgCl_2$, 5% v/v glycerol, 0–0.5 mM L-glutamine, 0–0.02 mM chorismate, and 9 μg ml^{-1} of the recombinant plant enzyme. The presence of an excess of *Ec*ADCL (20 μg ml^{-1}, 600 nM) is required for the production of pABA. Reactions (final volume 80 μl) were run in 96-well microplates (Greiner), and changes in fluorescence were continuously monitored with a microplate scanning spectrophotometer Safir^2 (Tecan). To monitor glutamate production, an excess of GDH (100 μg ml^{-1}, 4.2 units ml^{-1}) and 1 mM NAD were added to the assay, and NADH production was followed by its emission at 450 nm (excitation 340 nm). Concentration of pABA was monitored by its fluorescence emission at 340 nm (excitation 290 nm) in the presence of *Ec*ADCL.

The activities of GMPS and AS (β- plus α-subunits) were measured monitoring glutamate production. In both conditions, the final volume was 500 μl. For GMPS, the assay medium contained the following: 200 μM XMP, 1 mM ATP, 0.5 mM L-glutamine, 10 μg GMPS, 1 mM NAD, 4.2 units ml^{-1} GDH. For AS, the assay medium contained the following: 50 μM chorismate, 0.5 mM L-glutamine, 10 μg each of α- and β-subunits, 1 mM NAD, 4.2 units ml^{-1} GDH and various concentrations of rubreserine. The reactions were started by addition of glutamine, and the change in absorbance at 340 nm was monitored with a UV-visible spectrophotometer (Safas).

High Throughput Screening—The screening was conducted at the Center for the Screening of Bio-Active Molecules located

at the Commissariat à l'Energie Atomique-Grenoble, France. The library of compounds was purchased from The Prestwick Chemical Library®. This library contains 1200 molecules selected for their high chemical and pharmacological diversity. They are marketed and 100% Food and Drug Administration-approved compounds, supplied in the library at a 10 mM concentration in DMSO. The final concentration used in the enzymatic assay was 100 μM, and we verified in separate control experiments that 2% DMSO had no effect on the activity. The enzymatic test used for primary and secondary screenings was identical to the one described above for the GAT activity. Quality of the assay was assessed based on the calculation of the Z′ factor, as defined by Zhang *et al.* (35). After optimization of the assay, the Z′ factor was 0.76 ± 0.08 (a good assay must display a Z′ factor of >0.5). The assay was conducted as follows: 50 μl of a mixture containing 0.1 M Tris (pH 8), 5 mM $MgCl_2$, 5% glycerol, 40 μM chorismate, 1 mM NAD, 0.4 unit of GDH, 0.7 μg of GAT-ADCS, and 100 μM of the various molecules were added in each well (in control wells, molecules were omitted). The reaction was started by injection in each well of 30 μl of a solution containing 1.3 mM Gln, and the fluorescence changes (excitation 340 nm and emission 450 nm) were recorded at 0, 15, and 25 min. The most promising molecules were purchased, and their inhibitory properties were manually confirmed.

Measurements of Metabolites—Determinations of folates and pABA were essentially performed as described previously (36–38). Briefly, the extract corresponding to 3–5 × 10^7 parasites or 0.5 g (fresh weight) of plant material was subjected to separation using UPLC (for folates) or HPLC (for pABA), followed by tandem mass spectrometric detection on an API 4000 (Applied Biosystems, Foster City, CA), using electrospray ionization, in the multiple reaction monitoring mode. For folates, the final quantitative data reflect the sum of six different folate monoglutamates as follows: tetrahydrofolate (THF), 5-methyl-THF, 10-formyl-folic acid, 5,10-methenyl-THF, folic acid, and 5-formyl-THF (5-FTHF). [^{13}C]Folate derivatives and 3-NH_2-4-CH_3-benzoic acid were added in the extraction buffers as internal standards for folates and pABA, respectively.

RESULTS

GAT-ADCS Assay, High Throughput Screening, and GAT-ADCS Inhibition—The search for enzyme inhibitors by global approaches requires methods to determine the activity that are accurate, robust, and compatible with the automated platforms used for screening of chemical libraries. When coupled with GDH, GAT activity was easily measurable with a UV-visible spectrophotometer (340 nm) or a fluorimeter (excitation 340 nm and emission 450 nm) monitoring NADH accumulation (19, 39). Also, it was convenient to use the same procedure to test the inhibitors on GDH alone and to discard molecules that were specific for this last activity. Based on this protocol, we designed a miniature assay easily reproducible and optimized for the identification of active drugs, with a screening coefficient Z′ (a statistical parameter measuring the quality of the screening assay (35)) of 0.76 ± 0.08 (see "Experimental Procedures"). Because all our attempts to produce active recombinant GAT-ADCS from apicomplexan parasites failed, we used the recombinant plant enzyme as a model for this bifunctional

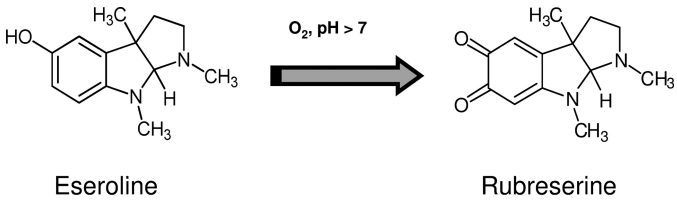

Eseroline Rubreserine

FIGURE 2. **Chemical structures of eseroline and rubreserine.** Oxidation of eseroline into rubreserine is spontaneous and strongly increased at pH >7.

system. We screened the registered Prestwick® Chemical Library (1200 compounds) against the GAT activity of the plant GAT-ADCS. After primary and secondary screenings, we identified only four molecules exhibiting IC_{50} values that were below 50 μM. They were manually tested, and we found that rubreserine (1,3*a*,8-trimethyl-1,2,3,3*a*,8,8*a*-hexahydropyrrolo[2,3-*b*]indole-5,6-dione, an oxidative product of eseroline (40–42) that spontaneously forms at alkaline pH (Fig. 2 and supplemental Fig. S1)) exhibited the best inhibitory properties. Eseroline itself had no effect, indicating that the carbonyl functions resulting from eseroline oxidation were essential for the inhibition. The rate constant of inhibition was rather low (about 0.1 min^{-1}), and a 20-min period of incubation with rubreserine was required to obtain maximal inhibition. We observed GAT-ADCS inhibition independently of the presence or position of the His tag that was added for purification convenience, indicating that such a tag was not involved in the inhibition process. We previously showed that the GAT activity was maximal in the presence of chorismate (the substrate of the ADCS domain) but could also operate independently (19). We observed inhibition of glutamate production in both conditions, *i.e.* with and without chorismate, and we also observed inhibition of pABA synthesis when GAT-ADCS was coupled with non limiting amounts of ADC lyase (Fig. 3, *A* and *B*). In separate control experiments, we verified that rubreserine did not impact ADC lyase activity. In all situations, rubreserine decreased the V_m and increased the K_m for glutamine, indicating a mixed type inhibition (Fig. 3*C*). Apparent equilibrium constants K_i (representing the ratio [*E*][I]/[*E*I], where *E* is enzyme; I is inhibitor; and S is substrate) and αK_i (representing the ratio [*ES*][I]/[*ES*I]) calculated from such pattern of curves (43) were estimated to be respectively 3 ± 1 and 8 ± 1 μM in the different conditions, *i.e.* measuring either glutamate or pABA productions.

In Vivo Effects of Rubreserine on A. thaliana Growth and Folate Content—When *Arabidopsis* seedlings were grown on agar plates in the presence of rubreserine concentrations ranging from 50 to 100 μM, we observed a dose-dependent growth inhibition (Fig. 4). Interestingly, when the agar plates were supplemented with pABA, the growth was restored for inhibitor concentrations up to 50 μM and partially restored for higher concentrations, the maximal effect being obtained with pABA concentrations ≥100 μM (Fig. 4). This suggests that for low rubreserine concentrations, at least, the growth inhibition was due to a limitation of pABA synthesis. Because pABA is required for folate biosynthesis, we also measured the potential impact of 5-FTHF on rubreserine-treated plants (Fig. 4). As shown, this folate derivative had similar effect than pABA.

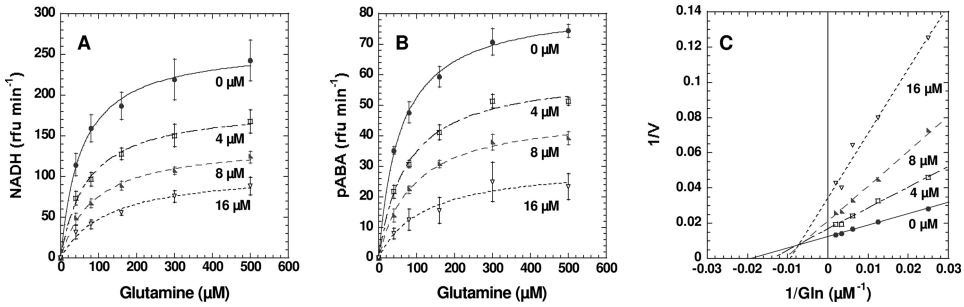

FIGURE 3. **Effect of rubreserine on GAT-ADCS kinetics.** *A,* glutamine-dependent glutamate production (GAT activity alone, no chorismate) in the presence of rubreserine. GAT-ADCS was first incubated with the various concentrations of rubreserine for 20 min, and then the kinetic was started by the addition of Gln, NAD, and GDH. *B,* glutamine-dependent pABA production (GAT-ADCS activity, 100 μM chorismate) in the presence of rubreserine and nonlimiting amount of ADCL. GAT-ADCS was first incubated with the various concentrations of rubreserine for 20 min, and then the kinetic was started by the addition of Gln, chorismate, and ADCL. *rfu*, relative fluorescence unit. *C,* reverse plot of *B*. Maximal rates of the recombinant enzyme were 140 ± 40 nmol min^{-1} mg^{-1} for GAT activity (glutamate production, no chorismate) and 130 ± 30 nmol min^{-1} mg^{-1} for GAT-ADCS activity (pABA production, with chorismate and ADCL). *Curves* were fitted with the hyperbolic equation of Michaelis-Menten (*A* and *B*) and linear regression (*C*). All our assays were made in triplicate and expressed ± S.D.

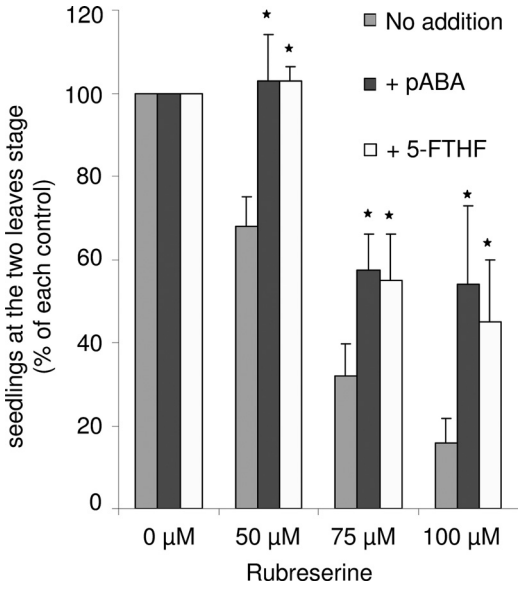

FIGURE 4. **Effect of rubreserine on the development of *Arabidopsis* seedlings.** Seedlings were grown in agar plates without (controls) or with 50, 75, or 100 μM rubreserine. The estimated number of seedlings at the rosette stage after 2 weeks is expressed as % of the conditions without rubreserine. The presence in the culture medium of 200 μM pABA or 200 μM 5-FTHF partially reversed the growth inhibition. Results are the average of at least three independent experiments ± S.D. *Asterisks* mark datasets showing statistical difference with the condition containing rubreserine alone in a Student's *t* test ($p < 0.05$).

TABLE 1

Effect of rubreserine (Rubre) on the folate content of *Arabidopsis* cells and comparison with sulfanilamide (Sulfa)

Cells were cultivated for 7 days with the various compounds before folate determinations. The total folate contents of control cells cultivated with or without 100 μM pABA were 11.8 ± 2 and 10 ± 1.5 nmol g^{-1} fresh weight, respectively. Measurements are the average ± S.D. of 4–6 determinations from two to three independent set of experiments. Results for each set of experiment are expressed as % *versus* the corresponding control.

Conditions	Total folates
	% versus control
Rubre 25 μM	60 ± 10
Rubre 25 μM + pABA 100 μM	85 ± 9
Rubre 50 μM	66 ± 3
Rubre 50 μM + pABA 100 μM	116 ± 12
Rubre 100 μM	54 ± 9
Sulfa 25 μM	42 ± 3
Sulfa 100 μM	39 ± 6

TABLE 2

Effect of rubreserine (Rubre) on the pABA contents of *Arabidopsis* cells and comparison with sulfanilamide (Sulfa)

Cells were cultivated for 7 days with the various compounds before pABA determination. The total and free pABA concentrations found in control cells were 8.5 ± 2 and 1.1 ± 0.4 nmol g^{-1} fresh weight. respectively. Measurements are the average ± S.D. of eight determinations from four sets of experiments. Results for each set of experiments are expressed as % *versus* the corresponding control.

Conditions	pABA	
	Total	Free
	% versus control	
Rubre 100 μM	90 ± 5	73 ± 8
Sulfa 100 μM	128 ± 16	132 ± 18

Next, we investigated the effect of rubreserine on the folate content. We used *Arabidopsis* cell cultures for these experiments to dispose of enough material for metabolite determinations. For rubreserine concentrations within the range 25–100 μM, the cell division came to an arrest after about 7 days. Similar results were obtained in the presence of sulfanilamide, a well known specific inhibitor of DHPS that blocks pABA utilization in the folate pathway (Fig. 1*A*). After 7 days, the pools of folate in rubreserine- and sulfanilamide-treated cells (Table 1) decreased by about 40 and 60%, respectively. However, the distributions of folate derivatives were not markedly modified (in all situations, the various representative pools of folates were roughly 50% 5-methyl-THF, 35% 10-formyl-THF plus 5,10-methenyl-THF, 8% 5-FTHF, 7% THF plus 5,10-methylene-THF, and 0.3% folic acid (30)). Interestingly, when 100 μM pABA were present in the culture medium, the folate content in both control and rubreserine-treated cells were almost identical (Table 1), which was clearly indicative of a protective effect of pABA. Because rubreserine inhibited the pABA branch of the folate pathway, we also attempted to measure the pABA content of *Arabidopsis* cells. In plants, pABA was found either as free acid or as a glucose ester conjugate. This last form (>80% of total pABA) is sequestered in vacuoles and does not directly contribute to folate synthesis (44, 45). This makes the determination of free pABA quite difficult because, as previously shown (44), breakdown of the esterified form of folate during sample workup is very difficult to avoid and contributes, sometimes quite significantly, to the amount of free pABA. However, in the presence of 100 μM rubreserine, we observed a small but significant decrease of free pABA by about 30% (Table 2). In contrast, the total amount of pABA did not markedly change, suggesting that the glucose ester conjugate in the vacuole and the free acid

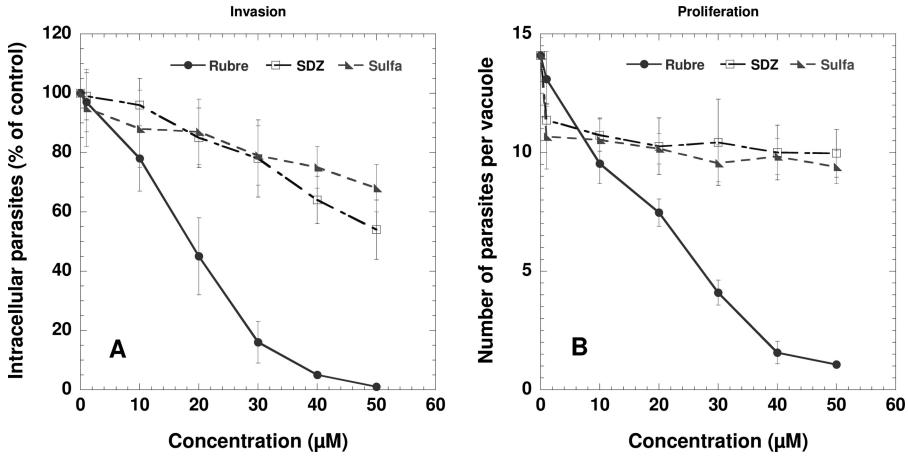

FIGURE 5. **Effect of rubreserine (*Rubre*) on invasion and proliferation of *T. gondii* and comparison with sulfanilamide (*Sulfa*) and sulfadiazine (*SDZ*).** *A,* invasion of human fibroblasts. The parasites were first incubated with the various drugs for 5 h and then placed in contact with HFF cells for 15 min. The number of intracellular parasites is expressed for each experiment as % of the number recorded in nontreated cells. *B,* intracellular growth of the parasites. Proliferation was estimated 24 h after the invasion process and expressed as the number of parasites present in the parasitophorous vacuoles. Results from invasion and proliferation experiments are the average of three to four independent experiments ± S.D.

form in the cytosol are not in rapid equilibrium. In sulfanilamide-treated cells, free and total pABA slightly increased by about 30% (Table 2), an expected result taking into account that pABA utilization was blocked (46).

Effect of Rubreserine on the Proliferation of Apicomplexan Parasites—Before testing the effect of rubreserine on *T. gondii*, we first verified with the [3-(4,5-dimethylthiazol-2-yl)-2,5-diphenyltetrazolium bromide] cytotoxicity assay (47) that rubreserine concentrations up to 50 μM had no toxicity on confluent HFF cells. Indeed, after 48 h of exposure to 50 μM rubreserine, the cell viability was still 95 ± 5% of the control. We then evaluated the effect of rubreserine on *Toxoplasma* parasites in two different situations as follows: invasion of confluent HFF by the parasites on the one hand, and intracellular development of the parasites within confluent HFF on the other hand. As shown in Fig. 5*A*, invasion of human cells strongly decreased when the parasites had been previously incubated with rubreserine. This effect was dose-dependent, and the number of intracellular parasites were reduced 2-fold in the presence of 20 μM rubreserine (IC_{50}). Likewise, when infected cells were placed in the presence of the inhibitor, the number of parasites in parasitophorous vacuoles decreased after 24 h in comparison with untreated infected cells, which was indicative of a slowing down of the parasite's intracellular division (Fig. 5*B*). In both situations, rubreserine appeared much more efficient than sulfanilamide and sulfadiazine, and this last sulfonamide drug was widely used in the treatment of toxoplasmosis. To correlate the inhibitory effect with folate biosynthesis, we attempted to determine the folate concentration in *T. gondii* cells. To our knowledge, there was no report about the intracellular concentration of folates within proliferating *T. gondii* parasites. We measured folates in parasites grown for 24 h in HFF cells placed in the presence of either 20 or 40 μM rubreserine (Table 3). Interestingly, in both conditions the total folate concentration decreased by a factor of 2. Also, similar to what was observed in plants, the distributions of folate derivatives were not significantly changed in the presence of the drug (in these cells the various representative pools of folates were as follows: 18% 5-methyltetrahydrofolate; 25% 10-formyltetrahydrofolate plus 5,10-methenyl-tetrahydrofolate; 42% 5-FTHF; 8% tetrahydrofolate plus 5,10-methylene-tetrahydrofolate; and 7% folic acid). In addition, for a rubreserine concentration of 20 μM (IC_{50} value), the parasite growth was largely restored in the presence of either pABA or 5-FTHF (Fig. 6*A*), and the maximal protective effect was obtained for concentrations ≥25 μM. Thus, for such inhibitor concentration (20 μM), the inhibitory process largely relied on the inhibition of pABA and folate biosynthesis. However, for rubreserine concentrations higher than 20 μM, pABA and 5-FTHF had only little effect (Fig. 6*B*), suggesting that high concentrations of the inhibitor had other non-folate-specific actions. Because antifolate drugs (anti-DHPS and anti-DHFR) are often used in combination, we tested the effect of rubreserine in combination with an anti-DHFR (Fig. 6*C*). When 20 μM rubreserine and 0.4 μM pyrimethamine were combined, the inhibition was slightly but significantly increased compared with rubreserine alone. Interestingly, rubreserine alone appeared in our experimental conditions as efficient as a mixture combining 50 μM sulfadiazine and 0.4 μM pyrimethamine.

TABLE 3

Effect of rubreserine (Rubre) on the folate content of *T. gondii* cells

Parasites were grown for 24 h in confluent HFF cells in the presence of 20 or 40 μM rubreserine. The results are expressed as nmol/10^7 parasites. Measurements are the average ± S.D. of two (40 μM Rubre), three (20 μM Rubre), and four (control) independent set of experiments.

Conditions	Total folates
	nmol/10⁷ parasites
No drug	10.2 ± 2.6
Rubre 20 μM	3.8 ± 1
Rubre 40 μM	4 ± 2

Additionally, rubreserine was also tested on the *in vitro* proliferation of *P. falciparum*. As shown in Fig. 7, rubreserine exhibited anti-malarial properties because the intraerythrocytic growth of the parasite was strongly inhibited by rubreserine, with an IC_{50} of 1 ± 0.04 μM ($n = 5$). Whether folate biosynthesis is also a primary target in these organisms is currently under investigation.

Specificity of Inhibition by Rubreserine—At low rubreserine concentrations, folate biosynthesis appeared as a main target in

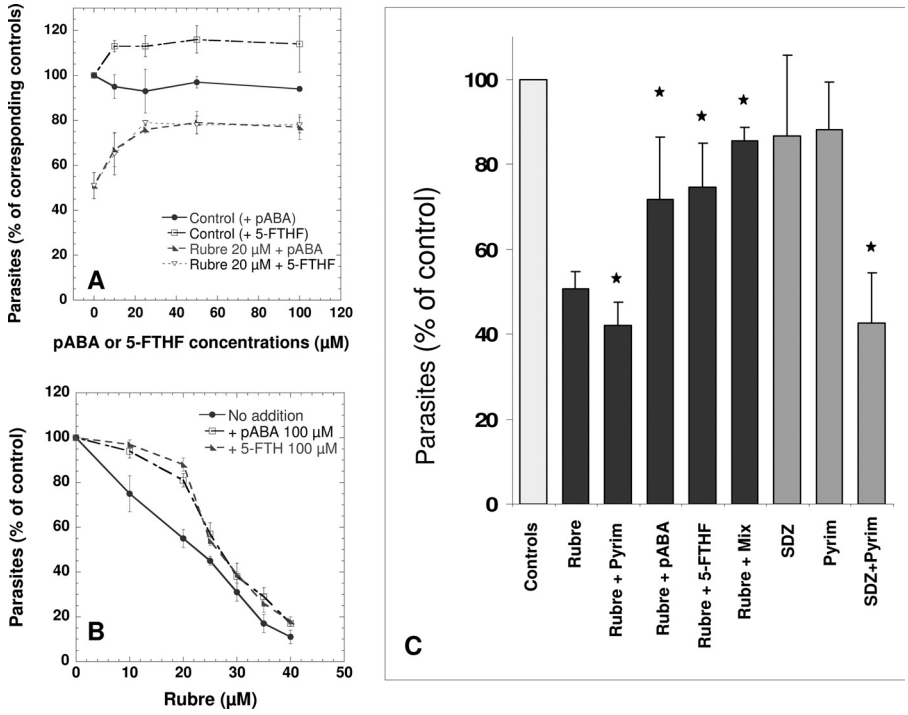

FIGURE 6. **Effect of rubreserine in combination with various other compounds on the proliferation of *T. gondii*.** The number of parasites present in the parasitophorous vacuoles after 24 h are expressed as % *versus* the corresponding controls (*i.e.* no addition, or pABA alone, or 5-FTHF alone). *A,* reverse effect of pABA and 5-FTHF in the presence of 20 μM rubreserine (*Rubre*). *B,* reverse effect of pABA and 5-FTHF (100 μM each) as a function of rubreserine concentration. *C,* effect of various drug combinations; the concentrations used were as follows: 20 μM rubreserine; 0.4 μM pyrimethamine (*Pyrim*); 100 μM pABA; 100 μM 5-formyltetrahydrofolate (*5-FTHF*); 50 μM sulfadiazine. *Mix* is a mixture containing pABA, anthranilate, UMP, and GMP at 50 μM each. *Asterisks* indicate statistical difference in a Student's *t* test ($p < 0.05$) between the conditions rubreserine alone and rubreserine in combination with other drugs, and between the conditions sulfadiazine or pyrimethamine alone and sulfadiazine plus pyrimethamine. Results are the averages of three independent experiments ± S.D.

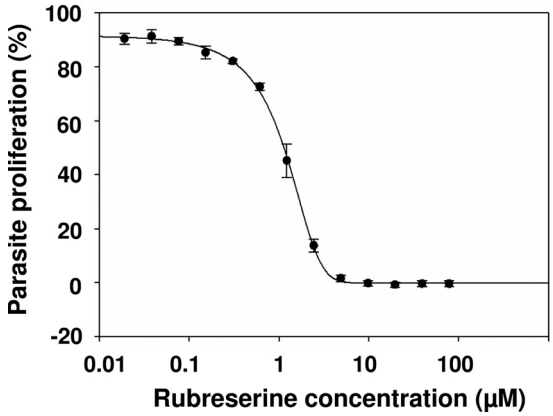

FIGURE 7. **Effect of rubreserine on the growth of *P. falciparum*.** Parasites were maintained under normal culture conditions and exposed to serial dilutions of rubreserine from 10 mM, and parasite proliferation was determined as a measurement of DNA content with SYBR Green I fluorescence after 96 h of exposure. Data are averaged from five independent experiments performed in triplicate (± S.D.).

TABLE 4

Effect of rubreserine on the GAT activities associated with recombinant *Arabidopsis* GAT-GMPS, AS, and GAT-ADCS

Activities were estimated measuring the glutamate production through a GDH-coupled assay, as described under "Experimental Procedures." Rubreserine concentrations up to 50 μM had no detectable effect on GDH activity alone. Assays were made in triplicate and expressed ± S.D.

Enzymes	Specific activity	IC_{50}
	$\mu mol\ min^{-1}\ mg^{-1}$	μM
*At*GAT-GMPS	0.30	25 ± 10
*At*AS (α- + β-subunits)	0.16	7 ± 2
*At*GAT-ADCS	0.40	8 ± 2
GDH (type II from bovine liver)	44	Not measurable, ≫50

Arabidopsis and *Toxoplasma*. However, at high rubreserine concentrations, the growth activity could not be fully restored by the presence of pABA or 5-FTHF, raising the question of the inhibitor specificity. GAT-ADCS belongs to the family of class I glutamine amidotransferases (18, 48), which contains six other members. The GAT domain of GAT-ADCS does not share strong homologies with the GAT domains of the other members of this class, and the best scores were obtained with AS (about 28% identity) GMPS (about 13% identity) and carbamoyl phosphate synthetase II (involved in UMP synthesis, about 15% identity). To test the effect of rubreserine on other members of this group, we attempted to produce these recombinant *Arabidopsis* activities. We failed to produce active recombinant carbamoyl-phosphate synthetase, but we produced AS (a heterodimeric protein combining the activities of β- and α-subunits, respectively, equivalent to TrpG and TrpE in prokaryotes (49)) and GMPS (a bifunctional enzyme with fused GAT and synthase domains (50), like GAT-ADCS). We determined these activities with the same GDH-coupled assay that we used for GAT-ADCS. As shown in Table 4, rubreserine also inhibited GMPS and AS activities, although inhibition of GMPS required higher concentrations of inhibitor. *Toxoplasma*, but not *Plasmodium,* is an auxotroph for tryptophan because of the lack of AS activity (51, 52). However, the enzymes involved in the synthesis of GMP (GMPS, a bifunctional enzyme, as in plants (53)) and UMP (carbamoyl-phosphate synthetase II, a heterodimer in plants (54), but a single protein in apicomplexan

parasites (55)) was present in these organisms. When a mixture containing pABA, anthranilate, UMP, and GMP (50 μM each) was added to the culture medium of rubreserine-treated plants or was present in the proliferation assay of *Toxoplasma*, the growth recovery for both organisms was not markedly improved compared with that obtained with pABA or 5-FTHF alones (see Fig. 6*B* for the experiments with *T. gondii*).

DISCUSSION

Two main conclusions can be drawn from this study: first, our data validate for the first time the use of the bifunctional GAT-ADCS as an efficient drug target in eukaryotic cells, and second, we identified a new scaffold that inhibits plant growth and proliferation of apicomplexan parasites.

The screening test we used appeared efficient to select active compounds from Prestwick® chemical library, and we found that an oxidative product of eseroline, rubreserine, was inhibiting the GAT activity of *At*GAT-ADCS. Eseroline and rubreserine were identified a long time ago as metabolites of physostigmine (eserine), an alkaloid present in the Calabar bean (*Physostigma venenosum*), and previously used for its potent anticholinesterase activity. To our knowledge, rubreserine and eseroline have no current use in any medical purpose. Pharmacological studies indicated that these two molecules were poor inhibitors of cholinesterase (56), but there was no reports indicating that rubreserine could affect folate biosynthesis and inhibit the growth of plants and the proliferation of parasites. Thus, we describe for this compound a new biological effect with interesting therapeutic potentialities.

When GAT-ADCS was coupled with ADC lyase, the apparent constant of inhibition (K_i) for pABA formation was estimated to be <10 μM, which is the best constant of inhibition obtained so far for the biosynthesis of pABA. How rubreserine affects the protein activity is not yet understood, however, and is currently under investigation. The obvious difference between the chemical structures of eseroline and rubreserine is the presence of two carbonyl functions on the aromatic ring of the latter compound. Thus, these carbonyl functions were presumably at the origin of the inhibitory effect. It must be noted that many other natural quinonoid compounds were shown to display antimalarial properties (57), although the targets and modes of action were not described for most of them.

The rubreserine-dependent growth inhibitions of *Arabidopsis* and *Toxoplasma* were specifically associated with an inhibition of folate biosynthesis for concentrations $\leq IC_{50}$, although higher concentrations might also inhibit other activities. The correlation between rubreserine and folate biosynthesis was observed by direct and indirect approaches. The direct approach indicated that *Arabidopsis* cells exhibited folate and free pABA contents lowered by 45 and 25%, respectively, in the presence of the inhibitor. In addition, when pABA was present in the culture medium of rubreserine-treated plant cells, the folate level was almost identical to the control, indicating a protective role of pABA. Likewise, the folate level in *Toxoplasma* cells was two times lowered by rubreserine. The impact of rubreserine on folate biosynthesis was also shown indirectly. Indeed, for rubreserine concentrations close to the IC_{50} values, the rubreserine-dependent growth inhibitions of *Arabidopsis* and *Toxoplasma* were for a large part reversed by the addition of pABA or 5-FTHF, indicating that the biosynthesis of pABA displayed a particular sensitivity to rubreserine and that the resulting decrease of folate biosynthesis contributed to the inhibitory process. The mode of action of rubreserine in *Plasmodium* is currently under investigation to determine to what extent folate biosynthesis is inhibited in this organism and the contribution of such an inhibition to the whole inhibitory process.

It is interesting to compare the effects of GAT-ADCS and DHPS inhibitors because both types of drugs impact pABA metabolism. Interestingly, rubreserine appeared in our experimental conditions much more efficient against *T. gondii* than sulfadiazine, a sulfonamide widely used for the treatment of severe toxoplasmosis. Indeed, the IC_{50} value calculated for rubreserine was significantly lower than the IC_{50} for sulfadiazine estimated from this study (>50 μM). The IC_{50} for sulfadiazine may fluctuate widely depending on the parasite strain, from about 20 μM to more than 200 μM, and is generally >30 μM (58). Such a variation presumably illustrates the occurrence of resistance within the numerous *Toxoplasma* strains. Sulfonamide drugs are normally not used alone against parasites of the Apicomplexa phylum because of their limited activity (8). However, they are potent synergizers of DHFR inhibitors (exemplified in Fig. 6*B*), which is the reason why these molecules are used in combination. Indeed, inhibition of DHPS decreases the *de novo* synthesis of dihydropteroate, which, in turn, leads to reduction of dihydrofolate, the substrate of DHFR. Because the amount of dihydrofolate is decreased, the efficiency of DHFR inhibitors increases, and lower doses of these toxic molecules are required. When rubreserine was used in combination with pyrimethamine in *Toxoplasma*, we also observed a small but significant synergistic effect, and such an association appeared as efficient as a mixture combining sulfadiazine and pyrimethamine. Thus, molecules with a hexahydropyrrolo[2,3-*b*]indole-5,6-dione scaffold, such as rubreserine, could be interesting structures to develop novel drugs that could represent alternatives to sulfonamides.

Acknowledgments—We thank Bernadette Gambonnet for technical assistance, Dr. Céline Richefeu-Contesto for helpful discussions, and Drs. Stéphane Ravanel and Claude Alban for critical reading of the manuscript.

REFERENCES

1. Rébeillé, F., Ravanel, S., Jabrin, S., Douce, R., Storozhenko, S., and Van Der Straeten, D. (2006) Folates in plants. Biosynthesis, distribution, and enhancement. *Physiol. Plant.* **126,** 330–342
2. Blancquaert, D., Storozhenko, S., Loizeau, K., De Steur, H., De Brouwer, V., Viaene, J., Ravanel, S., Rébeillé, F., Lambert, W., and Van Der Straeten, D. (2010) Folates and folic acid. From fundamental research toward sustainable health. *Crit. Rev. Plant Sci.* **29,** 14–35
3. Ravanel, S., Douce, R., and Rébeillé, F. (2011) in *Advances in Botanical Research* (Rébeillé, F., and Douce, R., eds) Vol. 59, pp. 67–106, Elsevier, Amsterdam, The Netherlands
4. Storozhenko, S., De Brouwer, V., Volckaert, M., Navarrete, O., Blancquaert, D., Zhang, G. F., Lambert, W., and Van Der Straeten, D. (2007) Folate fortification of rice by metabolic engineering. *Nat. Biotechnol.* **25,** 1277–1279

5. Díaz de la Garza, R. I., Gregory, J. F., 3rd, and Hanson, A. D. (2007) Folate biofortification of tomato fruit. *Proc. Natl. Acad. Sci. U.S.A.* **104,** 4218–4222
6. Rébeillé, F., Alban, C., Bourguignon, J., Ravanel, S., and Douce, R. (2007) The role of plant mitochondria in the biosynthesis of coenzymes. *Photosynth. Res.* **92,** 149–162
7. Bertino, J. R. (2009) Cancer research. From folate antagonism to molecular targets. *Best Pract. Res. Clin. Haematol.* **22,** 577–582
8. Nzila, A. (2006) Inhibitors of *de novo* folate enzymes in *Plasmodium falciparum*. *Drug Discov. Today* **11,** 939–944
9. Wang, P., Wang, Q., Aspinall, T. V., Sims, P. F., and Hyde, J. E. (2004) Transfection studies to explore essential folate metabolism and antifolate drug synergy in the human malaria parasite *Plasmodium falciparum*. *Mol. Microbiol.* **51,** 1425–1438
10. Wang, P., Wang, Q., Yang, Y., Coward, J. K., Nzila, A., Sims, P. F., and Hyde, J. E. (2010) Characterization of the bifunctional dihydrofolate synthase-folylpolyglutamate synthase from *Plasmodium falciparum*; a potential novel target for antimalarial antifolate inhibition. *Mol. Biochem. Parasitol.* **172,** 41–51
11. Nzila, A., Ward, S. A., Marsh, K., Sims, P. F., and Hyde, J. E. (2005) Comparative folate metabolism in humans and malaria parasites (part II). Activities as yet untargeted or specific to *Plasmodium*. *Trends Parasitol.* **21,** 334–339
12. Rattanachuen, W., Jönsson, M., Swedberg, G., and Sirawaraporn, W. (2009) Probing the roles of nonhomologous insertions in the N-terminal domain of *Plasmodium falciparum* hydroxymethylpterin pyrophosphokinase-dihydropteroate synthase. *Mol. Biochem. Parasitol.* **168,** 135–142
13. Hyde, J. E. (2005) Exploring the folate pathway in *Plasmodium falciparum*. *Acta Trop.* **94,** 191–206
14. Salcedo-Sora, J. E., Ochong, E., Beveridge, S., Johnson, D., Nzila, A., Biagini, G. A., Stocks, P. A., O'Neill, P. M., Krishna, S., Bray, P. G., and Ward, S. A. (2011) The molecular basis of folate salvage in *Plasmodium falciparum*. Characterization of two folate transporters. *J. Biol. Chem.* **286,** 44659–44668
15. Siehl, D. (1999) in *Plant Amino Acids* (Singh, B. K., ed) pp. 171–204, Marcel Dekker, Inc., New York
16. Roux, B., and Walsh, C. T. (1992) *p*-Aminobenzoate synthesis in *Escherichia coli*. Kinetic and mechanistic characterization of the amidotransferase PabA. *Biochemistry* **31,** 6904–6910
17. Basset, G. J., Quinlivan, E. P., Ravanel, S., Rébeillé, F., Nichols, B. P., Shinozaki, K., Seki, M., Adams-Phillips, L. C., Giovannoni, J. J., Gregory, J. F., 3rd, and Hanson, A. D. (2004) Folate synthesis in plants. The *p*-aminobenzoate branch is initiated by a bifunctional PabA-PabB protein that is targeted to plastids. *Proc. Natl. Acad. Sci. U.S.A.* **101,** 1496–1501
18. Zalkin, H. (1993) The amidotransferases. *Adv. Enzymol. Relat. Areas Mol. Biol.* **66,** 203–309
19. Camara, D., Richefeu-Contesto, C., Gambonnet, B., Dumas, R., and Rébeillé, F. (2011) The synthesis of pABA. Coupling between the glutamine amidotransferase and aminodeoxychorismate synthase domains of the bifunctional aminodeoxychorismate synthase from *Arabidopsis thaliana*. *Arch. Biochem. Biophys.* **505,** 83–90
20. Ziebart, K. T., and Toney, M. D. (2010) Nucleophile specificity in anthranilate synthase, aminodeoxychorismate synthase, isochorismate synthase, and salicylate synthase. *Biochemistry* **49,** 2851–2859
21. Kerbarh, O., Bulloch, E. M., Payne, R. J., Sahr, T., Rébeillé, F., and Abell, C. (2005) Mechanistic and inhibition studies of chorismate-utilizing enzymes. *Biochem. Soc. Trans.* **33,** 763–766
22. Bulloch, E. M., Jones, M. A., Parker, E. J., Osborne, A. P., Stephens, E., Davies, G. M., Coggins, J. R., and Abell, C. (2004) Identification of 4-amino-4-deoxychorismate synthase as the molecular target for the antimicrobial action of (6*S*)-6-fluoroshikimate. *J. Am. Chem. Soc.* **126,** 9912–9913
23. Kozlowski, M. C., Tom, N. J., Seto, C. T., Sefler, A. M., and Bartlett, P. A. (1995) Chorismate-utilizing enzymes isochorismate synthase, anthranilate synthase, and *p*-aminobenzoate synthase. Mechanistic insight through inhibitor design. *J. Am. Chem. Soc.* **117,** 2128–2140
24. Payne, R. J., Bulloch, E. M., Toscano, M. M., Jones, M. A., Kerbarh, O., and Abell, C. (2009) Synthesis and evaluation of 2,5-dihydrochorismate analogues as inhibitors of the chorismate-utilizing enzymes. *Org. Biomol. Chem.* **7,** 2421–2429
25. Payne, R. J., Bulloch, E. M., Kerbarh, O., and Abell, C. (2010) Inhibition of chorismate-utilizing enzymes by 2-amino-4-carboxypyridine and 4-carboxypyridone and 5-carboxypyridone analogues. *Org. Biomol. Chem.* **8,** 3534–3542
26. Ziebart, K. T., Dixon, S. M., Avila, B., El-Badri, M. H., Guggenheim, K. G., Kurth, M. J., and Toney, M. D. (2010) Targeting multiple chorismate-utilizing enzymes with a single inhibitor. Validation of a three-stage design. *J. Med. Chem.* **53,** 3718–3729
27. Dixon, S., Ziebart, K. T., He, Z., Jeddeloh, M., Yoo, C. L., Wang, X., Lehman, A., Lam, K. S., Toney, M. D., and Kurth, M. J. (2006) Aminodeoxychorismate synthase inhibitors from one-bead one-compound combinatorial libraries. "Staged" inhibitor design. *J. Med. Chem.* **49,** 7413–7426
28. Riedlinger, J., Reicke, A., Zähner, H., Krismer, B., Bull, A. T., Maldonado, L. A., Ward, A. C., Goodfellow, M., Bister, B., Bischoff, D., Süssmuth, R. D., and Fiedler, H. P. (2004) Abyssomicins, inhibitors of the *para*-aminobenzoic acid pathway produced by the marine Verrucosispora strain AB-18-032. *J. Antibiot.* **57,** 271–279
29. Keller, S., Schadt, H. S., Ortel, I., and Süssmuth, R. D. (2007) Action of atrop-abyssomicin C as an inhibitor of 4-amino-4-deoxychorismate synthase PabB. *Angew. Chem. Int. Ed. Engl.* **46,** 8284–8286
30. Loizeau, K., De Brouwer, V., Gambonnet, B., Yu, A., Renou, J. P., Van Der Straeten, D., Lambert, W. E., Rébeillé, F., and Ravanel, S. (2008) A genome-wide and metabolic analysis determined the adaptive response of *Arabidopsis* cells to folate depletion induced by methotrexate. *Plant Physiol.* **148,** 2083–2095
31. Bisanz, C., Bastien, O., Grando, D., Jouhet, J., Maréchal, E., and Cesbron-Delauw, M. F. (2006) *Toxoplasma gondii* acyl-lipid metabolism. *De novo* synthesis from apicoplast-generated fatty acids *versus* scavenging of host cell precursors. *Biochem. J.* **394,** 197–205
32. Allen, R. J., and Kirk, K. (2010) *Plasmodium falciparum* culture. The benefits of shaking. *Mol. Biochem. Parasitol.* **169,** 63–65
33. Bennett, T. N., Paguio, M., Gligorijevic, B., Seudieu, C., Kosar, A. D., Davidson, E., and Roepe, P. D. (2004) Novel, rapid, and inexpensive cell-based quantification of antimalarial drug efficacy. *Antimicrob. Agents Chemother.* **48,** 1807–1810
34. Smilkstein, M., Sriwilaijaroen, N., Kelly, J. X., Wilairat, P., and Riscoe, M. (2004) Simple and inexpensive fluorescence-based technique for high-throughput antimalarial drug screening. *Antimicrob. Agents Chemother.* **48,** 1803–1806
35. Zhang, J. H., Chung, T. D., and Oldenburg, K. R. (1999) A simple statistical parameter for use in evaluation and validation of high throughput screening assays. *J. Biomol. Screen.* **4,** 67–73
36. Zhang, G. F., Mortier, K. A., Storozhenko, S., Van De Steene, J., Van Der Straeten, D., and Lambert, W. E. (2005) Free and total *para*-aminobenzoic acid analysis in plants with high performance liquid chromatography/tandem mass spectrometry. *Rapid Commun. Mass Spectrom.* **19,** 963–969
37. De Brouwer, V., Zhang, G. F., Storozhenko, S., Straeten, D. V., and Lambert, W. E. (2007) pH stability of individual folates during critical sample preparation steps in prevision of the analysis of plant folates. *Phytochem. Anal.* **18,** 496–508
38. De Brouwer, V., Storozhenko, S., Stove, C. P., Van Daele, J., Van der Straeten, D., and Lambert, W. E. (2010) Ultra-performance liquid chromatography-tandem mass spectrometry (UPLC-MS/MS) for the sensitive determination of folates in rice. *J. Chromatogr. B Analyt. Technol. Biomed. Life Sci.* **878,** 509–513
39. Sahr, T., Ravanel, S., Basset, G., Nichols, B. P., Hanson, A. D., and Rébeillé, F. (2006) Folate synthesis in plants. Purification, kinetic properties, and inhibition of aminodeoxychorismate synthase. *Biochem. J.* **396,** 157–162
40. Poobrasert, O., Chai, H., Pezzuto, J. M., and Cordell, G. A. (1996) Cytotoxic degradation product of physostigmine. *J. Nat. Prod.* **59,** 1087–1089
41. Yang, S. T., Wilken, L. O., and Clark, C. R. (1987) Liquid chromatographic determination of the pH-dependent degradation of eseroline. Hydrolysis product of physostigmine. *J. Pharm. Biomed. Anal.* **5,** 383–393
42. Robinson, B. (1965) Structure of rubreserine. A decomposition product of physostigmine. *J. Pharm. Pharmacol.* **17,** 89–91
43. Segel, I. H. (1975) *Enzyme Kinetics*, John Wiley & Sons, Inc., New York
44. Quinlivan, E. P., Roje, S., Basset, G., Shachar-Hill, Y., Gregory, J. F., 3rd,

and Hanson, A. D. (2003) The folate precursor *p*-aminobenzoate is reversibly converted to its glucose ester in the plant cytosol. *J. Biol. Chem.* **278,** 20731–20737
45. Eudes, A., Bozzo, G. G., Waller, J. C., Naponelli, V., Lim, E. K., Bowles, D. J., Gregory, J. F., 3rd, and Hanson, A. D. (2008) Metabolism of the folate precursor *p*-aminobenzoate in plants. Glucose ester formation and vacuolar storage. *J. Biol. Chem.* **283,** 15451–15459
46. Orsomando, G., Bozzo, G. G., de la Garza, R. D., Basset, G. J., Quinlivan, E. P., Naponelli, V., Rébeillé, F., Ravanel, S., Gregory, J. F., 3rd, and Hanson, A. D. (2006) Evidence for folate-salvage reactions in plants. *Plant J.* **46,** 426–435
47. Mosmann, T. (1983) Rapid colorimetric assay for cellular growth and survival. Application to proliferation and cytotoxicity assays. *J. Immunol. Methods* **65,** 55–63
48. Massière, F., and Badet-Denisot, M. A. (1998) The mechanism of glutamine-dependent amidotransferases. *Cell. Mol. Life Sci.* **54,** 205–222
49. Zhang, X. H., Brotherton, J. E., Widholm, J. M., and Portis, A. R. (2001) Targeting a nuclear anthranilate synthase α-subunit gene to the tobacco plastid genome results in enhanced tryptophan biosynthesis. Return of a gene to its pre-endosymbiotic origin. *Plant Physiol.* **127,** 131–141
50. Nakamura, J., Straub, K., Wu, J., and Lou, L. (1995) The glutamine hydrolysis function of human GMP synthetase. Identification of an essential active-site cysteine. *J. Biol. Chem.* **270,** 23450–23455
51. Sibley, L. D., Messina, M., and Niesman, I. R. (1994) Stable DNA transformation in the obligate intracellular parasite *Toxoplasma gondii* by complementation of tryptophan auxotrophy. *Proc. Natl. Acad. Sci. U.S.A.* **91,** 5508–5512
52. Roberts, C. W., Roberts, F., Lyons, R. E., Kirisits, M. J., Mui, E. J., Finnerty, J., Johnson, J. J., Ferguson, D. J., Coggins, J. R., Krell, T., Coombs, G. H., Milhous, W. K., Kyle, D. E., Tzipori, S., Barnwell, J., Dame, J. B., Carlton, J., and McLeod, R. (2002) The shikimate pathway and its branches in apicomplexan parasites. *J. Infect. Dis.* **185,** S25-S36
53. Bhat, J. Y., Shastri, B. G., and Balaram, H. (2008) Kinetic and biochemical characterization of *Plasmodium falciparum* GMP synthetase. *Biochem. J.* **409,** 263–273
54. Schröder, M., Giermann, N., and Zrenner, R. (2005) Functional analysis of the pyrimidine *de novo* synthesis pathway in solanaceous species. *Plant Physiol.* **138,** 1926–1938
55. Fox, B. A., and Bzik, D. J. (2002) *De novo* pyrimidine biosynthesis is required for virulence of *Toxoplasma gondii*. *Nature* **415,** 926–929
56. Ellis, S., Krayer, O., and Plachte, F. L. (1943) Studies on physostigmine and related substances. III. Breakdown products of physostigmine; their inhibitory effect on cholinesterase and their pharmacological action. *Pharmacol. Exp. Ther.* **79,** 309–319
57. Kaur, K., Jain, M., Kaur, T., and Jain, R. (2009) Antimalarials from nature. *Bioorg. Med. Chem.* **17,** 3229–3256
58. Meneceur, P., Bouldouyre, M. A., Aubert, D., Villena, I., Menotti, J., Sauvage, V., Garin, J. F., and Derouin, F. (2008) *In vitro* susceptibility of various genotypic strains of *Toxoplasma gondii* to pyrimethamine, sulfadiazine, and atovaquone. *Antimicrob. Agents Chemother.* **52,** 1269–1277

Inhibition of *p*-Aminobenzoate and Folate Syntheses in Plants and Apicomplexan Parasites by Natural Product Rubreserine

Djeneb Camara, Cordelia Bisanz, Caroline Barette, Jeroen Van Daele, Esmare Human, Bernice Barnard, Dominique Van Der Straeten, Christophe P. Stove, Willy E. Lambert, Roland Douce, Eric Maréchal, Lyn-Marie Birkholtz, Marie-France Cesbron-Delauw, Renaud Dumas and Fabrice Rébeillé

J. Biol. Chem. 2012, 287:22367-22376.
doi: 10.1074/jbc.M112.365833 originally published online May 10, 2012
